Research Article

Cancer Immunology Research

Regression of Metastatic Merkel Cell Carcinoma Following Transfer of Polyomavirus-Specific T Cells and Therapies Capable of Reinducing HLA Class-I

Aude G. Chapuis[1], Olga K. Afanasiev[3,4], Jayasri G. Iyer[4], Kelly G. Paulson[3,4], Upendra Parvathaneni[8], Joo Ha Hwang[9], Ivy Lai[1], Ilana M. Roberts[1], Heather L. Sloan[1], Shailender Bhatia[7], Kendall C. Shibuya[1], Ted Gooley[1], Cindy Desmarais[10], David M. Koelle[2,4,5,6,11], Cassian Yee[1], and Paul Nghiem[3,4]

Abstract

Merkel cell carcinoma (MCC) is an aggressive skin cancer that typically requires the persistent expression of Merkel cell polyomavirus (MCPyV) oncoproteins that can serve as ideal immunotherapeutic targets. Several immune evasion mechanisms are active in MCC, including downregulation of HLA class-I expression on tumor cells and dysfunctional endogenous MCPyV-specific CD8 T-cell responses. To overcome these obstacles, we combined local and systemic immune therapies in a 67-year-old man, who developed metastatic MCPyV-expressing MCC. Intralesional IFN-β-1b or targeted single-dose radiation was administered as a preconditioning strategy to reverse the downregulation of HLA-I expression noted in his tumors and to facilitate the subsequent recognition of tumor cells by T cells. This was followed by the adoptive transfer of *ex vivo* expanded polyclonal, polyomavirus-specific T cells as a source of reactive antitumor immunity. The combined regimen was well tolerated and led to persistent upregulation of HLA-I expression in the tumor and a durable complete response in two of three metastatic lesions. Relative to historical controls, the patient experienced a prolonged period without development of additional distant metastases (535 days compared with historic median of 200 days; 95% confidence interval, 154–260 days). The transferred $CD8^+$ T cells preferentially accumulated in the tumor tissue, remained detectable and functional for more than 200 days, persisted with an effector phenotype, and exhibited evidence of recent *in vivo* activation and proliferation. The combination of local and systemic immune stimulatory therapies was well tolerated and may be a promising approach to overcome immune evasion in virus-driven cancers. *Cancer Immunol Res; 2(1); 27–36. ©2013 AACR.*

Introduction

Merkel cell carcinoma (MCC) represents a highly aggressive neuroendocrine skin malignancy with a high disease-associated mortality, early metastatic disease, and a high propensity for recurrence after initial treatment. The cause-specific mortality rate ranges from 23% to 80% at 5 years, thus making it three times as lethal as melanoma (1). The Merkel cell polyomavirus (MCPyV) is clonally integrated into at least 80% of MCC tumors and produces the viral T-antigen (T-Ag) oncoproteins that are persistently expressed by MCC and are necessary for the survival and proliferation of tumor cells (2–5). Compared with mammalian tumor-associated antigens (TAA) that all have some degree of expression within normal tissue, MCPyV T-Ag expression is restricted to MCC, is a foreign antigen not subject to T-cell self-tolerance mechanisms, and is thus an optimal target for immunotherapy. Because no viral particles are formed in the tumor cells, antiviral agents are inefficient (6).

As adoptive transfer has demonstrated clinical benefit for both viral and endogenous tumor antigens (7–9), we sought to apply the use of antigen-specific T cells to target the MCPyV large T-Ag (LT-Ag) oncoprotein. The HLA-A*2402-restricted MCPyV $LT\text{-}Ag_{92\text{-}101}$-specific T cells (hereafter referred to as MCPyV-specific cells) were identified in a patient with metastatic MCC (10). These MCPyV-specific T cells, when isolated from tumors or peripheral blood mononuclear cells (PBMC) of patients with MCC, are largely

Authors' Affiliations: [1]Program in Immunology; [2]Vaccine and Infectious Disease Division, Fred Hutchinson Cancer Research Center; Departments of [3]Pathology, [4]Medicine (Dermatology), [5]Laboratory Medicine, [6]Global Health, and [7]Medicine (Medical Oncology), University of Washington; Divisions of [8]Radiation Oncology and [9]Gastroenterology, University of Washington Medical Center; [10]Adaptive Biotechnologies; and [11]Benaroya Research Institute, Seattle, Washington

Note: Supplementary data for this article are available at Cancer Immunology Research Online (http://cancerimmunolres.aacrjournals.org/).

A.G. Chapuis and O.K. Afanasiev contributed equally to this work.

Current address for I. Lai and C. Yee: Melanoma Medical Oncology, MD Anderson Cancer Center, Houston, TX; current address for I.M. Roberts: Surgery Branch, NIH, Bethesda, MD.

Corresponding Authors: Paul Nghiem, Division of Dermatology, UWMC, 850 Republican Street, Box 358050, Seattle, WA 98195. Phone: 206-221-2632; Fax: 206-221-4394; E-mail: pnghiem@uw.edu; and Cassian Yee, Department of Melanoma Medical Oncology, Department of Immunology Unit 0430, MD Anderson Cancer Center, 1515 Holcombe Blvd. Unit 904, Houston, TX 77030. Phone: 713-563-5272; Fax: 713-563-3424; E-mail: cyee@mdanderson.org

doi: 10.1158/2326-6066.CIR-13-0087

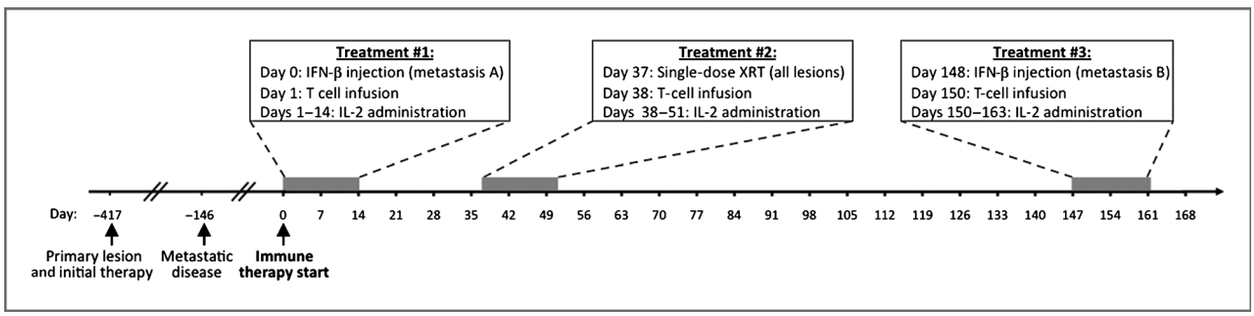

Figure 1. Timeline for disease presentation and immune therapy. Events as indicated relative to immune therapy start date. The patient received a total of three treatments that consisted of HLA-I upregulation (either intralesional injection of 3×10^6 IU of IFN-β-Ib or 8 Gy radiotherapy) followed by administration of $10^{10}/m^2$ MCPyV-specific polyclonal $CD8^+$ T cells and 14 days of twice-daily s.c. injections of IL-2 (2.5×10^5 IU/m^2). XRT, radiotherapy.

dysfunctional and exhibit an immune inhibitory ($PD\text{-}1^+$/$Tim3^+$) phenotypic profile (11). We hypothesized that *ex vivo* generation of polyclonal MCPyV-specific T cells might augment the probability of including and expanding cells that had an increased potential for proliferation, function, and persistence after transfer as evidenced in murine and nonhuman primate models (12, 13).

Similar to the observations in other virus-associated cancers, HLA class-I (HLA-I) downregulation is an immune escape mechanism present in the majority of MCC tumors (14–16). Single-dose low-dose radiation has been shown to upregulate cell surface HLA-I expression (17). Data from murine models suggest that single-dose radiation is more effective than fractionated radiation in promoting tumor immunity, because the latter may suppress the function of lymphocytes that are recruited to the tumor (18). Furthermore, IFNs direct the upregulation of HLA-I (19), and intralesional administration of IFN-β has been observed to promote immune responses in MCC (14, 20).

Here, we investigated whether adoptive transfer of polyclonal MCPyV-specific $CD8^+$ T-cells following HLA-I upregulation strategies (intralesional IFN-β or local, single-fraction radiotherapy) could safely establish persistent anti-MCC responses, migrate to tumor tissue, and induce regression of MCPyV-positive, HLA-I–deficient MCC metastases.

Case report

A 67-year-old man with chronic renal failure secondary to a nephrectomy for renal cell carcinoma (RCC) at the age of 50 presented with a 1.6-cm (in largest dimension) MCC lesion on his left upper thigh and a negative sentinel node biopsy (American Joint Committee on Cancer stage IA). He underwent a wide local excision followed by 50 Gy of fractionated local radiation to the primary site. Eight months later while still asymptomatic, a surveillance whole body positron emission tomography (PET) scan detected a 2.9×1.8 cm lesion adjacent to the pancreatic head. Merkel polyomavirus-specific CD8 T cells were identified in the patient's tumor-infiltrating lymphocytes (TIL) and peripheral blood using a MCPyV-tetramer (ref. 10; Supplementary Fig. S1). The patient underwent leukapheresis to allow MCPyV-specific T cells to be harvested. The patient was enrolled in a single-patient clinical trial of autologous T-cell therapy for MCC [Fred Hutchinson Cancer Research Center (FHCRC, Seattle, WA) protocol #2558]. Both the primary tumor and pretreatment metastasis were confirmed to be classical MCC by dot-like cytokeratin-20 staining. Both lesions expressed the MCPyV T-Ag, whereas HLA-I expression was absent or sparse. Two additional metastases in the pancreatic head and neck appeared 137 days before the initiation of therapy.

The patient underwent three rounds of treatment (Fig. 1). Intralesional IFN-β-Ib (3×10^6 IU) was first administered by endoscopic ultrasound-guided fine-needle injection to the largest of the three detectable pancreatic metastases (designated as metastasis A). After 24 hours, the patient received an infusion of $10^{10}/m^2$ MCPyV tetramer-specific polyclonal $CD8^+$ T cells followed by low-dose s.c. interleukin (IL)-2 (2.5×10^5 IU/m^2) twice daily for 14 days as a means to increase T-cell persistence (21). Thirty-seven days later, a single 8-Gy fraction of radiation was delivered to all three remaining lesions (designated as metastases A, B, and C) followed by a second infusion of $10^{10}/m^2$ MCPyV-specific $CD8^+$ T cells and low-dose s.c. IL-2. On day 148 after the first infusion, metastasis B was injected with IFN-β-1b followed by a third cell infusion and low-dose s.c. IL-2 × 14 days. The patient experienced low-grade fevers and a transient, less than 72-hour grade 1–2 lymphopenia after each infusion, consistent with the expected immediate toxicities associated with T-cell infusions (22, 23). No changes in end organ function, inflammation- or autoimmune-related complications were observed. As detailed in the Results section, follow-up scans showed no evidence of new distant disease until 535 days after the original pancreatic metastasis was detected. At that time, the patient developed new brain lesions that he declined to have worked up or treated. The patient died 1 month later without additional therapeutic interventions.

Materials and Methods

Clinical protocol and patient characteristics

All clinical investigations were conducted according to the Declaration of Helsinki principles. The single-patient protocol #2558 (described above) was approved by the FHCRC Institutional Review Board and the U.S. Food and Drug Administration. The patient provided written informed consent.

Isolation and expansion of MCC-specific CTLs

PBMCs were collected by leukapheresis and all ensuing *ex vivo* manipulations involving processing of products destined for infusion were performed in the cGMP Cell Processing Facility of the FHCRC based on a protocol established for *in vitro* enrichment of low frequency antigen-specific cytotoxic T lymphocytes (CTL; refs. 24, 25). To facilitate the isolation of antigen-specific CTL, PBMCs were depleted of $CD25^+$ T cells to eliminate regulatory T cells (Tregs; ref. 26; Miltenyi Biotec Inc.), and stimulated twice for 7 to 10 days with HLA-A^*2402-restricted MCPyV LT-$Ag_{92\text{-}101}$ peptide (CPC Scientific)-pulsed autologous dendritic cells. Each stimulation was supplemented with the γ_c-chain cytokines IL-2 (10 IU/mL), IL-7 (5 ng/mL), and IL-21 (30 ng/mL). Cultures that contained more than 5% specific $CD8^+$ T cells assessed by tetramer stains were clinical-grade sorted (BD Influx cell sorter, BD Biosciences) before expansion to sufficient numbers for infusion as previously described (21, 27, 28). Cell products bound the MCPyV LT-$Ag_{92\text{-}101}$ peptide-HLA tetramer, secreted IFN-γ, and lysed MCPyV LT-$Ag_{92\text{-}101}$-pulsed FUJI ($A24^+$ cell line) pulsed with 10 μg/mL peptide (Supplementary Fig. S2).

T-cell tracking by HLA-peptide tetramers

Tetramers (produced by the FHCRC immune monitoring core facility) were used to detect transferred MCPyV LT-$Ag_{92\text{-}101}$-specific $CD8^+$ T cells in PBMCs collected after infusions. The sensitivity of the tetramer is 0.05% of total $CD8^+$ T cells. Persistence after infusions was calculated as the last time point at which $tetramer^+$ T cells were detected at 2 × background levels or ≥0.05%.

Flow cytometry

Blood samples were collected at the indicated time points, and the PBMCs were isolated by Ficoll-Hypaque gradient and cryopreserved. Cells that bound tetramer were analyzed by flow cytometry after staining with fluorochrome-conjugated monoclonal antibodies to CD14, CD16, CD19 (dump channel), CD8, CD4, CD137, CD28, CD127, CD62L, CCR7, PD-1, and TIM-3 (BD-Pharmingen). Intracellular cytokine production of IFN-γ, TNF-α, and IL-2 by cells responding to *in vitro* stimulation with MCPyV LT-$Ag_{92\text{-}101}$ peptide for 4 to 5 hours were performed as described (29). Intranuclear expression of Ki-67 was assessed after permeabilization (eBioscience). Cells were analyzed on an LSRII cytometer (Becton Dickinson) using FACS-Diva software. Multiparametric flow cytometry staining, acquisition, and analyses were performed on all samples in a batch on the same day and one negative control for each parameter was used. As the percentages of $tetramer^+$ T cells in the samples are often low, this method dedicated the majority of the PBMC for sample analyses.

Tracking polyclonal T cells using high-throughput TCR-β chain DNA sequencing

A pool of primers to all V and J pairs specifically designed to amplify the complete VDJ junction region, was designed such that only the minimal region (60 nucleotides) containing the antigen-specific nucleotide information for each T-cell receptor (TCR)-β CDR3 could be amplified and sequenced using the immunoSEQ assay (Adaptive Biotechnologies; ref. 30). Using genomic DNA isolated from the blood and tumor samples as a template, this method was used to capture the frequency of individual TCRs in biologic samples with accurate reproducibility and a sensitivity of 1/100,000 TCR-containing lymphocytes (31, 32). DNA from the blood and tumor samples was prepared using the DNeasy Blood & Tissue Kit (Qiagen). The sources of available cells for DNA extraction include the tetramer-sorted infusion product, cryopreserved PBMC derived using Ficoll isolation, phytohemagglutinin and IL-2–expanded TIL isolated from the primary tumor, and freshly isolated cells from the pancreatic metastatic tumor biopsy following immune therapy treatment. The results of individual TCR clonotypes are expressed as a percentage of all productive, in-frame TCRs sequenced.

Immunohistochemistry

Anti-CD8 clone 4B11 (Novocastra), anti-MCPyV T-Ag (5), and anti-HLA-I clone EMR8-5 (MBL International) were used at 1:200, 1:4,000, and 1:200 dilutions, respectively, after heat-induced epitope retrieval. Specimens were assessed for MCPyV T-Ag and HLA-I expression and scored using the Allred method (33). An Allred score of 0 to 1.5 was considered negative (0), 2 to 5.5 weak (+), 6 to 7.5 moderate (++), and 8 strong (+++). Peritumoral and intratumoral CD8 infiltrates were scored separately as previously described (14). The numbers of $CD8^+$ cells were assessed and expressed on a 0-to-5 scale with a mean of 0, 90, 306, 508, 675, and 732+ CD8s/mm^2, respectively. Intratumoral CD8 lymphocytes were surrounded by tumor cells only with no visualized contact with stroma.

Statistical analysis

The observed time between the first metastasis and the second metastasis for 49 patients was available and these data were used as historic controls. All of these patients presented with local or regional disease (stage I, II, or III) and later developed distant metastatic disease, for which they then received treatment. The time between metastases was treated as a time-to-event endpoint, and from these controls, the median time to second metastasis was estimated along with a point-wise estimate of the 95% confidence interval for the median time. We only included a highly analogous patient population from our historical controls. Cases that would not be eligible for the trial were eliminated, including those with profound immune suppression and those who only had a single subsequent skin metastasis (these are often independent primary lesions or represent a very benign subset of patients). Statistical tests were performed with the GraphPad prism software version 3.0, with the R-package for statistical analysis (http://www.r-project.org), or SAS version 9.2.

Results

HLA-I upregulation followed by adoptive transfer of MCPyV-specific T cells induces regression of Merkel cell carcinoma

Pre- and posttreatment tumor tissue immunohistochemistry was used to evaluate viral oncoprotein expression, HLA-I expression, and CD8 lymphocyte infiltration (Fig. 2A). As

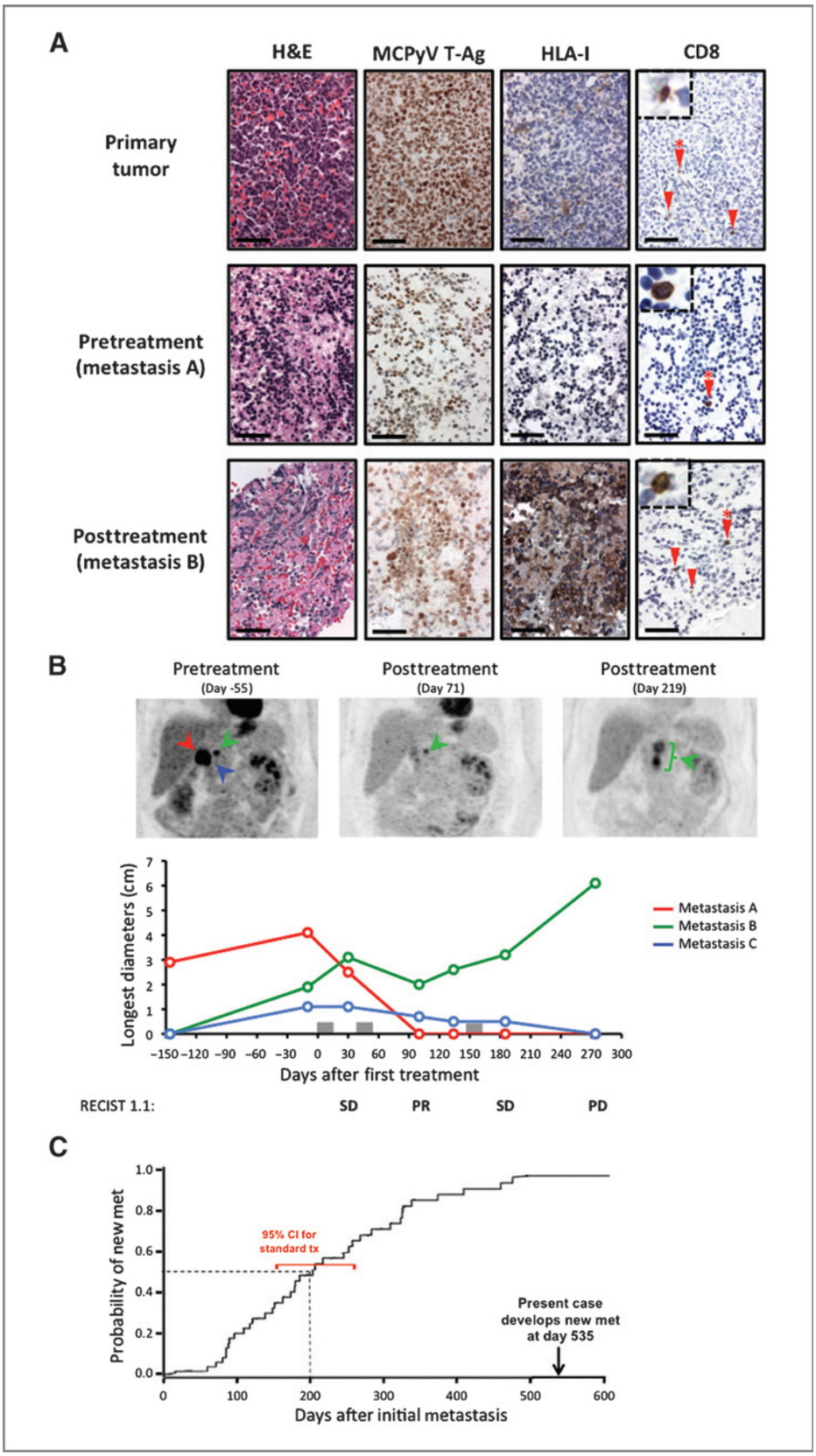

Figure 2. Response of individual MCC metastases after combined immune therapy. A, columns from left to right, hematoxylin and eosin (H&E) stains, immunohistochemistry for MCPyV T-Ag, HLA-I, and CD8 (red arrows, red asterisk indicates cell in the inset) of the primary tumor, pretreatment (metastasis A, biopsied immediately before start of immune therapy) and posttreatment (metastasis B, biopsied 148 days after start of immune therapy) tumors. Scale bar, 50 μm. B, MRI imaging (except the first datapoint, day 146, which was obtained by PET/CT) of individual metastases that included a peri-pancreatic lesion adjacent to the anterior duodenum (metastasis A, red), a pancreatic neck lesion (metastasis B, green), and a pancreatic head lesion (metastasis C, blue). The longest diameter in cm (*y*-axis) of each metastasis is graphed over time (*x*-axis). Representative images of pre- and posttreatment PET/CT scans are shown above the graph. Gray bars on *x*-axis indicate the timing of each treatment as detailed in Fig. 1. The corresponding RECIST 1.1 criteria are indicated below the graph. C, Kaplan–Meier curve of the probability of developing a second distant metastasis after the first detected metastasis (plotted at day zero) in 49 patients with MCC who developed distant disease. The 95% confidence interval is indicated in red.

anticipated, the primary tumor and pretreatment metastasis A biopsies were positive for the MCPyV T-Ag oncoprotein, but had weak or no HLA-I expression. In contrast, HLA-I was strongly upregulated on the biopsy of the posttreatment metastasis (metastasis B) taken 146 days after the first treatment cycle, and as expected, MCPyV T-Ag expression was persistently maintained. Scattered $CD8^+$ T-cell infiltrates were detected in the primary tumor, as well as in the pre- and posttreatment biopsies (Fig. 2A).

Tumor burden and clinical efficacy were monitored using MRI and PET/CT scans (Fig. 2B). Immediately before the first treatment, the patient's initial pancreatic metastasis had enlarged, and two adjacent pancreatic tumors were newly detected compared with the scan performed 146 days earlier. Restaging 30 days after the first treatment showed that the largest lesion, which had undergone injection with IFN-β-Ib, had decreased in size, but the other two lesions had remained stable or increased in size. The best overall response by Response Evaluation Criteria in Solid Tumors (RECIST) was a partial response observed following the second treatment consisting of localized, single-dose 8-Gy radiation before T-cell infusion and low-dose s.c. IL-2. After the third treatment, two of three lesions continued to regress and one lesion remained refractory to treatment.

To determine systemic effects of adoptively transferred T cells, the time for new metastasis to develop after treatment was assessed in comparison with 49 historical matched controls undergoing standard, typically cytotoxic chemotherapy (Fig. 2C). The patient showed no additional systemic metastasis until 535 days after the appearance of the first metastasis, which greatly exceeds the estimated median time of 200 days (95% confidence interval, 154–260 days) for development of new distant metastatic disease in historic controls. The scan performed 535 days after the initial metastasis revealed new brain lesions that the patient declined work-up. These likely represented MCC metastases; however, as the patient also had a history of remote RCC and no biopsy was performed, metastasis from an RCC origin could not be excluded. Overall, these data suggest the treatment-induced regression in two of three metastases and may have contributed to a delay in the development of new distant disease.

Enhanced ability to respond to antigen after transfer of virus-specific $CD8^+$ T cells

The frequency and persistence of MCPyV-specific CD8 T cells in peripheral blood were assessed by their ability to bind the MCPyV-specific tetramer (Fig. 3A, solid circles). The frequency of these cells peaked 4 to 7 days after infusions (up to 8.8% of total $CD8^+$ T cells) and remained detectable at the last assessment (219 days after the first treatment) at frequencies of approximately 1%, which corresponded to a more than 3-fold increase compared with preinfusion levels (0.26%).

We next assessed whether the virus-specific T cells detected after treatment were functional as assessed by their ability to secrete IFN-γ in response to cognate peptide. Before the treatment cycles, cells that secreted IFN-γ after exposure to the MCPyV peptide could not be detected within PBMC, suggesting that the MCPyV-specific cells binding to tetramer in the pretreatment PBMC were nonfunctional. However, the frequency of CD8 T cells that secreted IFN-γ in response to MCPyV peptide increased after each infusion (5.1, 4.5, and 3% after treatments 1, 2, and 3, respectively) and remained detectable at frequencies of 1% or more of total $CD8^+$ T cells up to 219 days after the first infusion (Fig. 3A, open circles). Furthermore, the frequency of MCPyV-reactive peptide-responsive $CD8^+$ T cells correlated closely with the frequency of MCPyV tetramer-positive cells, suggesting that most of the persisting virus-specific cells remained functional *in vivo*.

Because an increased frequency of virus-specific T cells over time may reflect antigen-specific cell division, we investigated whether the persisting MCPyV-specific T cells expressed Ki-67, a marker of proliferation (34). Before infusion, endogenous (preexisting) MCPyV-specific T cells did not express Ki-67, indicating minimal/absent proliferation. Cells from the infusion product were overwhelmingly positive for Ki-67 (92% at day 14 after the last stimulation cycle *in vitro*), consistent with recent activation. Most transferred cells maintained Ki-67 expression early after transfer (>80% on day 1 after infusion) and, as expected, Ki-67 expression decreased after each infusion but remained well above baseline levels (Fig. 3B, solid diamonds) 219 days after the first infusion. Ki-67 expression on MCPyV-specific CD8 T cells was overall significantly higher ($P \leq 0.005$) than Ki-67 expression of the host tetramer-negative CD8 Tcells (Fig. 3B, open diamonds), suggesting that the infused cells continued to divide in the presence of persistent antigen.

To validate the functional status and determine the differentiation profile of pre- and posttreatment virus-specific CD8 T cells, we evaluated the phenotype of the persisting transferred cells. Consistent with the absence of function and proliferation, both PD-1 (a marker of activation/exhaustion) and TIM-3 (a marker of exhaustion) were expressed on MCPyV-specific cells (90% and 78%, respectively) found in PBMC before the treatment cycles, suggesting endogenous CD8 responses were dysfunctional and exhausted (Fig. 3C and D). As expected, and following *ex vivo* expansion, the infusion product also expressed PD-1 (34%) and TIM-3 (93%). However, once infused into the patient, the transferred cells maintained PD-1 expression but lost Tim-3 expression such that cells found after transfer had a nonexhausted phenotype (Fig. 3C), consistent with their maintained function. Furthermore, 7 days after transfer, 53% of MCPyV-specific cells transiently expressed CD137 (4-1BB), a marker associated with very recent activation (Fig. 3E).

On the basis of the absence of expression of the costimulatory molecule CD28, the IL-7 receptor CD127 as well as the lymph node homing molecules, CD62L and CCR7 (data not shown), the endogenous MCPyV-specific T cells found before infusions exhibited a differentiated effector memory phenotype (Fig. 3F and G). Consistent with the use of IL-21 in the *ex vivo* cultures (24–26), a subset of the infusion product generated for this patient expressed CD28 (78%) and CD127 (19%). After infusion into the patient, the transferred cells maintained CD28 expression (Fig. 3F) and further upregulated CD127 (Fig. 3G). CD62L and CCR7 were not detected (data not shown).

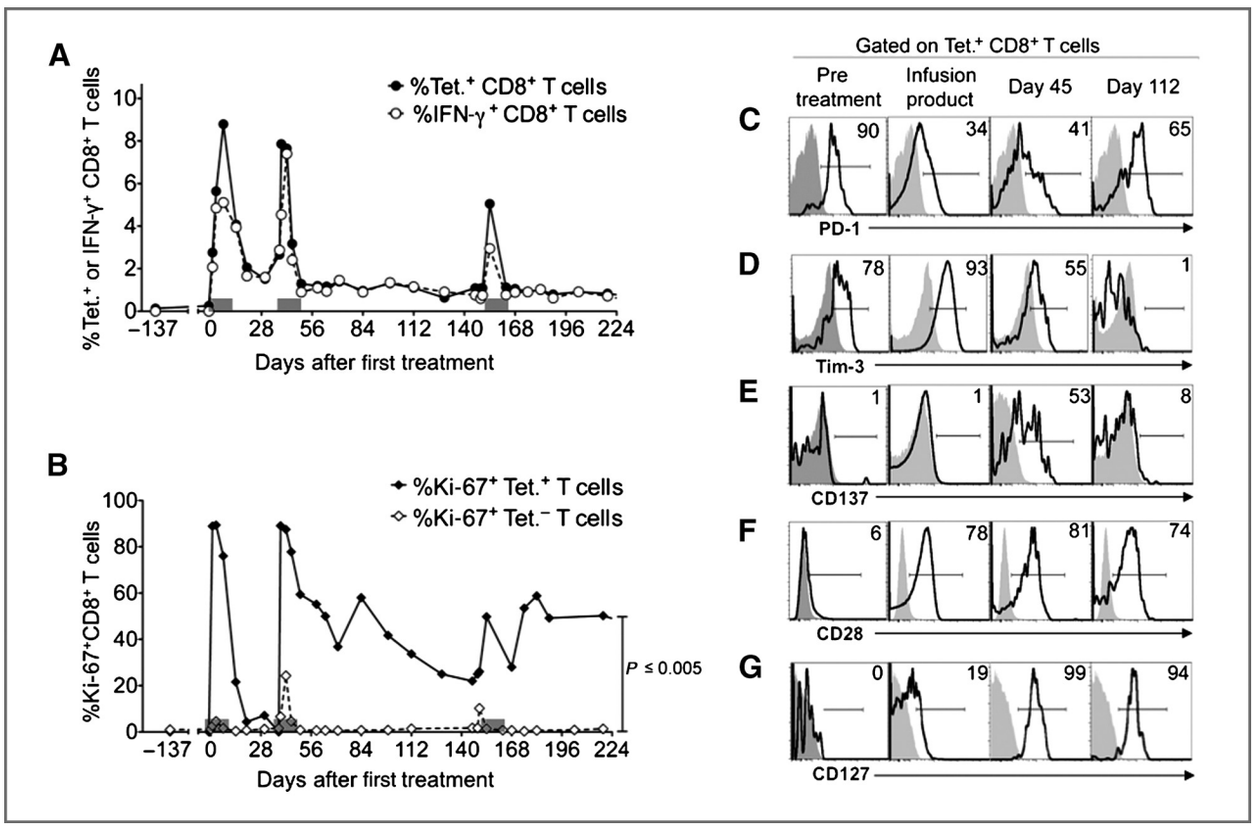

Figure 3. Persistence, function, and phenotype of transferred MCPyV-specific CD8$^+$ T cells. A, assessment of tetramer$^+$CD8$^+$ T cells (%, solid circles, solid line) and IFN-γ–reactive CD8$^+$ T cells (%, open circles, dashed line) in PBMC collected at baseline (137 days and immediately before the first treatment) and at indicated time points after treatments. Gray bars on *x*-axis indicate the timing of each treatment as detailed in Fig. 1. B, intranuclear Ki-67 expression on baseline and posttreatment CD8$^+$tetramer$^+$ cells (solid diamonds, solid line), and CD8$^+$tetramer$^-$ cells (open diamonds, dashed line). Gray bars on the *x*-axis indicated the timing of treatments as in A above. C–G, expression of PD-1, TIM-3, CD137, CD28, and CD127 on the infusion product, tetramer$^+$CD8$^+$ PBMC collected at baseline and after treatment as indicated. All parameters were acquired from multiple time points on the same day using the same negative control for each parameter as described in Materials and Methods, except for CD137 on day 45. A two-tailed paired *t* test was used for statistical analysis.

These data suggest that the transferred cells persisted with an effector memory phenotype (13), but in a less differentiated state compared with the endogenous response, with a maintained capacity to signal through CD28 and CD127. Tregs can be sensitive to exogenous IL-2, and could have a negative impact on the persistence and function of transferred cytotoxic lymphocytes. Therefore, we assessed Treg numbers after infusions based on the expression of surrogate markers CD4 and CD25 and the absence of CD127 (24). Treg frequencies increased after each infusion from baseline levels but returned to near baseline levels within 28 days of the infusion (Supplementary Fig. S3). In TIL, unfortunately, we were severely limited by the quantity of tissue available for analysis from the patient's metastases and therefore Treg analysis could not be performed.

Overall, adoptive transfer of polyclonal, MCPyV-specific T cells was associated with several key characteristics suggestive of an enhanced ability to respond to antigen: (i) markedly increased frequency of MCPyV-specific cells that persisted *in vivo*, (ii) increased fraction of virus-reactive T cells, (iii) ability to proliferate (Ki-67), (iv) expression of activation markers (CD137, PD-1), and (v) facilitated costimulation and survival (CD28 and CD127; refs. 35, 36).

Transferred cells preferentially localize to metastatic MCC tissue

To capture the number and characteristics of the individual transferred MCPyV-specific CD8$^+$ T-cell clones, we analyzed tetramer-sorted infusion products, TIL, and PBMC for individual TCR-β CDR3 using high-throughput TCR DNA sequencing (32). The infusion product (which was sorted a second time to yield >99% pure CD8$^+$ tetramer$^+$ cells for TCR-β CDR3 analysis) was polyclonal and consisted of 502 individual virus-specific clonotypes. Three clonotypes were predominant and represented 99% of MCPyV-specific TCR reads (all three clones shared V-β7-9 and differed by their J-β subunits as depicted in Fig. 4A and B). We then used this method to determine all TCR-β CDR3 present in unsorted TIL and PBMC obtained before and after infusions and investigated whether the transferred virus-specific clonotypes were present within these samples, as well as their frequency. Before treatment, these three J-β variant clones were present among primary tumor TIL (0.03% J-β1-5, 0.06% J-β1-1, 2.8% J-β2-3; Fig. 4C, left), and PBMC (0.06% J-β1-5, 0.15% J-β1-1, 0.01% J-β2-3; Fig. 4D, left), suggesting that these preexisting clonotypes had been expanded in the PBMC-derived infusion product. Analysis of the posttreatment

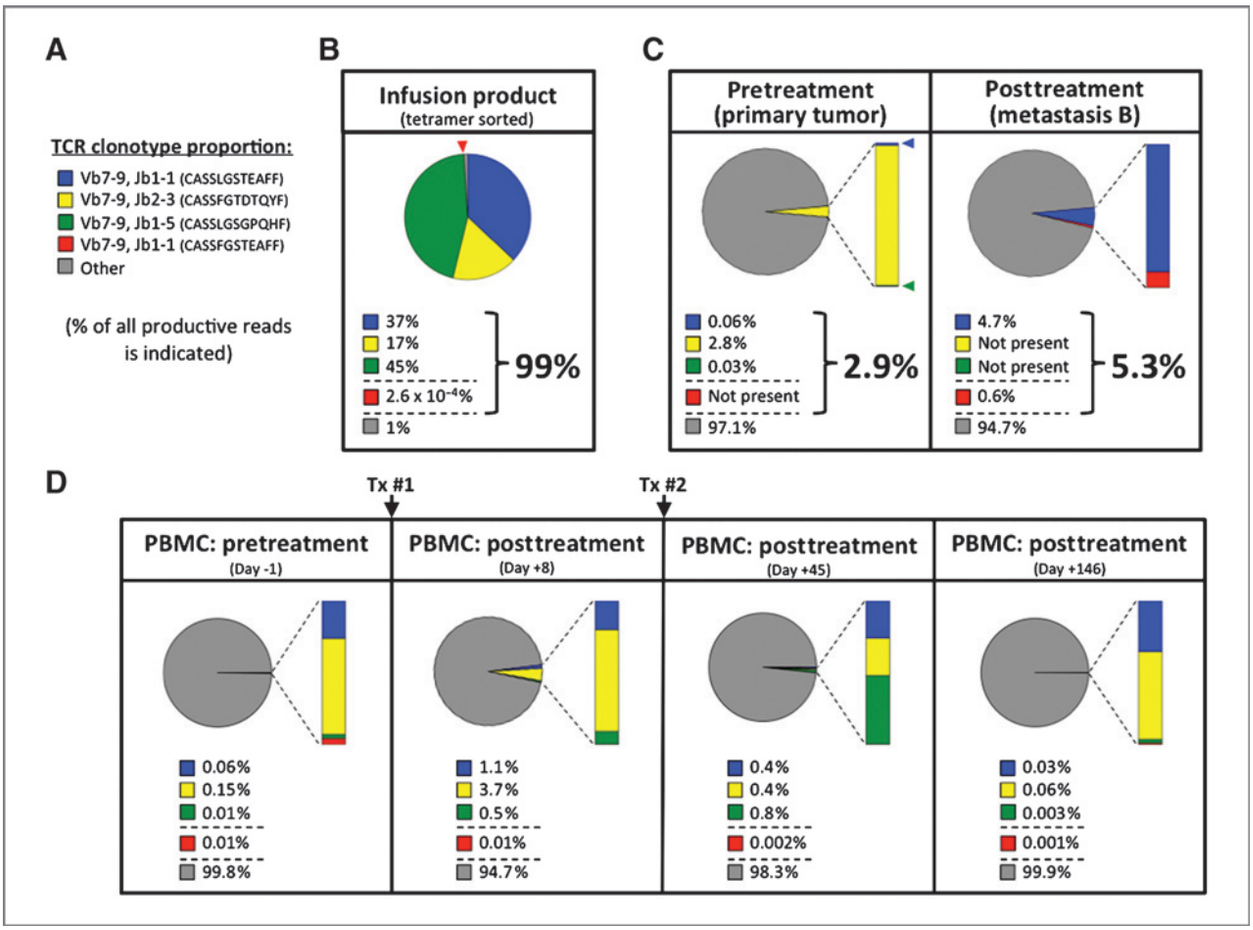

Figure 4. TCR clonotypic analysis for infused T cells and TIL within MCC tumors. A, legend for the four Vβ7-9 TCR clonotypes that were MCPyV-specific as assessed by HLA-A24–restricted MCPyV-specific tetramer binding. B, pie chart indicating the individual TCR-β CDR3 clonotypes composing the $CD8^+$ $tetramer^+$ MCPyV-specific T cells isolated from the infusion product. Gray indicates other clonotypes found in the tetramer-sorted infusion product. C, pie charts indicating the prevalence of the individual TCR-β CDR3 clonotypes present in the infusion product among all TCR-β CDR3 clonotypes isolated from expanded TIL from the primary tumor before treatment (left) and directly *ex vivo* from metastasis B after treatment (day +148, right). The relative percentages of the individual clones are indicated. Gray indicates all other clonotypes found in the biopsy sample. D, pie charts tracking the prevalence of the individual TCR-β CDR3 clonotypes among PBMC before and at several time points after treatment.

metastasis 146 days after the first infusion demonstrated that clone Jβ1-1 now represented 4.7% of all sequences, and the clones Jβ1-5 and Jβ2-3 were absent (Fig. 4C, right).

We then investigated whether additional clonotypes that were present in the posttreatment metastasis were also present within the low-prevalence MCPyV-specific clonotypes (<1%) in the infusion product. This analysis identified an additional MCPyV-specific clonotype (highlighted in red), with one nucleic-acid difference compared with the Jβ1-1 clonotype highlighted in blue that was present at 0.6% of all TCR reads in the posttreatment metastatic biopsy and absent in the pretreatment TIL. However, because the frequency in the infusion product was so low (2.6 × 10-4%), we cannot formally exclude that this clone constituted a contaminant.

Overall, MCPyV-specific CD8 T-cell clonotypes present in the infused product increased from 2.9% in the primary tumor to 5.3% in the postinfusion metastasis (Fig. 4C). Two clones accounted for the increase in MCPyV-specific cells present in the biopsy metastasis following the treatments compared with the primary lesion. No increase in frequency of these three clones was observed in the peripheral blood before and after treatments at comparable time points (Fig. 4D, right). Using this method, the specificity of the majority of the clonotypes isolated from PBMC and TIL could not be determined and may have included (i) T cells specific for other MCPyV epitopes; (ii) T cells recognizing nonviral TAAs such as survivin (37); HIP1 oncoprotein that interacts with c-KIT (38), CD56, or other UV-induced mutational signatures; or (iii) bystander or resident T cells. In summary, as the infusion product contained clones that aggregated at a higher frequency in the metastatic lesion compared with the peripheral blood, this suggests there was preferential localization of infused virus-specific T cells to the metastatic tissue.

Discussion

The purpose of this study was to investigate the efficacy and safety of HLA-I upregulating agents in combination with

polyomavirus-specific adoptive T-cell therapy in the setting of metastatic MCC. Even though preexisting MCPyV-specific $CD8^+$ T cells were present at low frequencies in the host before infusions (10), these were unable to prevent the rapid progression of metastatic disease. We addressed two key factors that may have contributed to the inefficiency of the endogenous virus-specific T-cell responses: To reverse the observed downregulated HLA-I expression on tumor cells necessary for the display of the MCPyV viral peptides, and render the cells accessible to specific T-cell lysis, either intralesional IFN-β-1b and tumor-targeted, single-dose ionizing radiation (8 Gy) was administered 1 to 2 days before each T-cell infusion. To address the absence of function of the endogenous CD8 responses, polyclonal MCPyV-specific CD8 T cells were generated *ex vivo* from PBMC, expanded, and reinfused. This resulted in the increased frequency of detectable and functional CD8 T cells for more than 3 months *in vivo* and preferential localization of the infused cells in tumor tissue as evidenced by TCR clonotype analysis. The combination of HLA-I upregulation followed by the infusion of MCPyV-specific CD8 T cells was well tolerated and safe and mediated tumor regression in two of three detectable metastases consistent with T-cell–mediated lysis. The absence of new metastatic disease in this patient for a prolonged period of time compared with historic controls also suggests that the treatment may have delayed or prevented the progression of distant metastatic disease. Although the patient declined definitive workup, it seems he developed metastatic MCC disease in the brain, a site with limited lymphocyte accessibility (39).

Although a clear increase in antitumor reactivity was achieved with this treatment, immune escape was not entirely halted. Although regressing lesions in the pancreas could not be biopsied, the escaping pancreatic lesion was amenable to a limited fine-needle aspirate. Our data indicate that HLA-I and MCPyV T-Ag expression were maintained on the escaping lesion, and thus their respective downregulation was eliminated as having played a role in immune evasion in the pancreas. Other mechanisms may have contributed to immune escape in some lesions in the patient. Infiltration of tumor tissue by $CD8^+$ T cells has been shown to have a positive effect on survival in numerous cancer settings. TIL density and distribution were shown to independently predict sentinel lymph node status and survival in patients with melanoma (40, 41). In MCC, a clear correlation between $CD8^+$ T-cell infiltration and favorable clinical outcome has been established, consistent with a role for the recognition of tumor cells by host T cells (14). In this patient, $CD8^+$ T-cell infiltration in the primary tumor and pre- and posttreatment metastatic lesions remained scarce, suggesting that other factors may have prevented $CD8^+$ infiltration and effective tumor lysis. A recent report suggests that vascular E-selectin within MCC tumors is critical in mediating intratumoral $CD8^+$ T-cell infiltration (42); however, the intratumoral vascular architecture could not be assessed in this case. Furthermore, PD-1 expression has been shown to be higher in the tumor-infiltrating $CD8^+$ T cells and is associated with disease progression (43–45). Although transferred cells were PD-1^+ and functional in the peripheral blood, the function of the $CD8^+$ T cells infiltrating the tumor could not be assessed. Ultimately, more effective results might also be achieved by combining adoptive transfer with immunomodulatory strategies such as blockade of the PD-1/PD-L1 axis or anti-CTLA-4 blockade (46–48).

Similar to other virus-driven cancers, MCC is an attractive target for immunotherapy because characterized, non-self, non-cross–reactive antigens are constitutively expressed and necessary for tumor survival (3). The results of this single-patient study suggest that immune-mediated antitumor activity can be established with a very limited side effect profile and offers a strategy to rapidly elucidate the requirements for MCC tumor control directly in humans by bypassing the necessity of murine models (49, 50). A multipatient clinical trial is currently under way (NCT01758458) to further test this combinatorial immunotherapy approach using additional viral CD8 T-cell epitopes in a broader cohort of patients with MCC.

Disclosure of Potential Conflicts of Interest

C. Desmarais has ownership interest (including patents) in Adaptive Biotechnologies. No potential conflicts of interest were disclosed by the other authors.

Authors' Contributions

Conception and design: A.G. Chapuis, O.K. Afanasiev, J.G. Iyer, K.G. Paulson, D.M. Koelle, C. Yee, P. Nghiem

Development of methodology: A.G. Chapuis, O.K. Afanasiev, J.G. Iyer, K.G. Paulson, D.M. Koelle, C. Yee

Acquisition of data (provided animals, acquired and managed patients, provided facilities, etc.): A.G. Chapuis, O.K. Afanasiev, J.G. Iyer, K.G. Paulson, J.H. Hwang, I. Lai, H.L. Sloan, S. Bhatia, K.C. Shibuya, C. Desmarais, C. Yee

Analysis and interpretation of data (e.g., statistical analysis, biostatistics, computational analysis): A.G. Chapuis, O.K. Afanasiev, K.G. Paulson, I.M. Roberts, S. Bhatia, T. Gooley, C. Desmarais, C. Yee, P. Nghiem

Writing, review, and/or revision of the manuscript: A.G. Chapuis, O.K. Afanasiev, K.G. Paulson, J.H. Hwang, H.L. Sloan, S. Bhatia, C. Yee, P. Nghiem

Administrative, technical, or material support (i.e., reporting or organizing data, constructing databases): K.G. Paulson, I.M. Roberts, H.L. Sloan, C. Desmarais, P. Nghiem

Study supervision: A.G. Chapuis, O.K. Afanasiev, C. Yee, P. Nghiem

Acknowledgments

The authors thank Dr. James A. DeCaprio for providing the MCPyV large T-Ag antibody Ab3.

The costs of publication of this article were defrayed in part by the payment of page charges. This article must therefore be hereby marked *advertisement* in accordance with 18 U.S.C. Section 1734 solely to indicate this fact.

Received June 29, 2013; revised October 24, 2013; accepted October 25, 2013; published OnlineFirst November 4, 2013.

References

1. Henness S, Vereecken P. Management of Merkel tumours: an evidence-based review. Curr Opin Oncol 2008;20:280–6.
2. Feng H, Shuda M, Chang Y, Moore PS. Clonal integration of a polyomavirus in human Merkel cell carcinoma. Science 2008;319:1096–100.
3. Houben R, Shuda M, Weinkam R, Schrama D, Feng H, Chang Y, et al. Merkel cell polyomavirus-infected Merkel cell carcinoma cells require expression of viral T antigens. J Virol 2010;84:7064–72.
4. Shuda M, Arora R, Kwun HJ, Feng H, Sarid R, Fernández-Figueras M-T, et al. Human Merkel cell polyomavirus infection I. MCV T antigen

expression in Merkel cell carcinoma, lymphoid tissues and lymphoid tumors. Int J Cancer 2009;125:1243–9.
5. Rodig SJ, Cheng J, Wardzala J, DoRosario A, Scanlon JJ, Laga AC, et al. Improved detection suggests all Merkel cell carcinomas harbor Merkel polyomavirus. J Clin Invest 2012;122:4645–53.
6. Hadrup S, Donia M, Thor Straten P. Effector CD4 and CD8 T cells and their role in the tumor microenvironment. Cancer Microenviron 2012; 6:123–33.
7. Chapuis AG, Thompson JA, Margolin KA, Rodmyre R, Lai IP, Dowdy K, et al. Transferred melanoma-specific CD8+ T cells persist, mediate tumor regression, and acquire central memory phenotype. Proc Natl Acad Sci U S A 2012;109:4592–7.
8. Heslop HE, Slobod KS, Pule MA, Hale GA, Rousseau A, Smith CA, et al. Long-term outcome of EBV-specific T-cell infusions to prevent or treat EBV-related lymphoproliferative disease in transplant recipients. Blood 2009;115:925–35.
9. Hunder NN, Wallen H, Cao J, Hendricks DW, Reilly JZ, Rodmyre R, et al. Treatment of metastatic melanoma with autologous CD4+ T cells against NY-ESO-1. N Engl J Med 2008;358:2698–703.
10. Iyer JG, Afanasiev OK, McClurkan C, Paulson K, Nagase K, Jing L, et al. Merkel cell polyomavirus-specific CD8(+) and CD4(+) T-cell responses identified in Merkel cell carcinomas and blood. Clin Cancer Res 2011;17:6671–80.
11. Afanasiev OK, Yelistratova L, Miller N, Nagase K, Paulson K, Iyer JG, et al. Merkel polyomavirus-specific T cells fluctuate with Merkel cell carcinoma burden and express therapeutically targetable PD-1 and Tim-3 exhaustion markers. Clin Cancer Res 2013;19:5351–60.
12. Wherry EJ, Teichgraber V, Becker TC, Masopust D, Kaech SM, Antia R, et al. Lineage relationship and protective immunity of memory CD8 T cell subsets. Nat Immunol 2003;4:225–34.
13. Berger C, Jensen MC, Lansdorp PM, Gough M, Elliott C, Riddell SR. Adoptive transfer of effector CD8+ T cells derived from central memory cells establishes persistent T cell memory in primates. J Clin Invest 2008;118:294–305.
14. Paulson KG, Iyer JG, Tegeder AR, Thibodeau R, Schelter J, Koba S, et al. Transcriptome-wide studies of Merkel cell carcinoma and validation of intratumoral CD8+ lymphocyte invasion as an independent predictor of survival. J Clin Oncol 2011;29:1539–46.
15. Haque M, Ueda K, Nakano K, Hirata Y, Parravicini C, Corbellino M, et al. Major histo-compatibility complex class I molecules are down-regulated at the cell surface by the K5 protein encoded by Kaposi's sarcoma-associated herpes virus/human herpesvirus-8. J Gen Virol 2001;82:1175–80.
16. Koopman LA, van Der Slik AR, Giphart MJ, Fleuren GJ. Human leukocyte antigen class I gene mutations in cervical cancer. J Natl Cancer Inst 1999;91:1669–77.
17. Reits EA, Hodge JW, Herberts CA, Groothuis TA, Chakraborty M, Wansley EK, et al. Radiation modulates the peptide repertoire, enhances MHC class I expression, and induces successful antitumor immunotherapy. J Exp Med 2006;203:1259–71.
18. Lee Y, Auh SL, Wang Y, Burnette B, Wang Y, Meng Y, et al. Therapeutic effects of ablative radiation on local tumor require CD8+ T cells: changing strategies for cancer treatment. Blood 2009; 114:589–95.
19. Boss JM. Regulation of transcription of MHC class II genes. Curr Opin Immunol 1997;9:107–13.
20. Nakajima H, Takaishi M, Yamamoto M, Kamijima R, Kodama H, Tarutani M, et al. Screening of the specific polyoma virus as diagnostic and prognostic tools for Merkel cell carcinoma. J Dermatol Sci 2009; 56:211–3.
21. Yee C, Thompson JA, Byrd D, Riddell SR, Roche P, Celis E, et al. Adoptive T cell therapy using antigen-specific CD8+ T cell clones for the treatment of patients with metastatic melanoma: in vivo persistence, migration, and antitumor effect of transferred T cells. Proc Natl Acad Sci U S A 2002;99:16168–73.
22. National Cancer Institute NIoH. Common Terminology Criteria for Adverse Events (CTCAE) v4.0. 10/01/2009 ed: Cancer Therapy Evaluation Program; 2009.
23. Ettinghausen SE, Moore JG, White DE, Platanias L, Young NS, Rosenberg SA. Hematologic effects of immunotherapy with lymphokine-activated killer cells and recombinant interleukin-2 in cancer patients. Blood 1987;69:1654–60.
24. Chapuis AG, Ragnarsson GB, Nguyen HN, Chaney CN, Pufnock JS, Schmitt TM, et al. Transferred WT1-reactive CD8+ T cells can mediate antileukemic activity and persist in post-transplant patients. Sci Transl Med 2013;5:174ra27.
25. Li Y, Bleakley M, Yee C. IL-21 influences the frequency, phenotype, and affinity of the antigen-specific CD8 T cell response. J Immunol 2005;175:2261–9.
26. Li Y, Yee C. IL-21 mediated Foxp3 suppression leads to enhanced generation of antigen-specific CD8+ cytotoxic T lymphocytes. Blood 2008;111:229–35.
27. Ho WY, Nguyen HN, Wolfl M, Kuball J, Greenberg PD. *In vitro* methods for generating CD8+ T-cell clones for immunotherapy from the naïve repertoire. J Immunol Methods 2006;310:40–52.
28. Riddell SR, Watanabe KS, Goodrich JM, Li CR, Agha ME, Greenberg PD. Restoration of viral immunity in immunodeficient humans by the adoptive transfer of T cell clones. Science 1992;257:238–41.
29. Papagno L, Almeida JR, Nemes E, Autran B, Appay V. Cell permeabilization for the assessment of T lymphocyte polyfunctional capacity. J Immunol Methods 2007;328:182–8.
30. Wang C, Sanders CM, Yang Q, Schroeder HW Jr, Wang E, Babrzadeh F, et al. High throughput sequencing reveals a complex pattern of dynamic interrelationships among human T cell subsets. Proc Natl Acad Sci U S A 2010;107:1518–23.
31. Robins H, Desmarais C, Matthis J, Livingston R, Andriesen J, Reijonen H, et al. Ultra-sensitive detection of rare T cell clones. J Immunol Methods 2012;375:14–9.
32. Robins HS, Campregher PV, Srivastava SK, Wacher A, Turtle CJ, Kahsai O, et al. Comprehensive assessment of T-cell receptor beta-chain diversity in alphabeta T cells. Blood 2009;114:4099–107.
33. Allred DC, Harvey JM, Berardo M, Clark GM. Prognostic and predictive factors in breast cancer by immunohistochemical analysis. Mod Pathol 1998;11:155–68.
34. Scholzen T, Gerdes J. The Ki-67 protein: from the known and the unknown. J Cell Physiol 2000;182:311–22.
35. Boise LH, Minn AJ, Noel PJ, June CH, Accavitti MA, Lindsten T, et al. CD28 costimulation can promote T cell survival by enhancing the expression of Bcl-XL. Immunity 1995;3:87–98.
36. Kimura MY, Pobezinsky LA, Guinter TI, Thomas J, Adams A, Park JH, et al. IL-7 signaling must be intermittent, not continuous, during CD8 (+) T cell homeostasis to promote cell survival instead of cell death. Nat Immunol 2013;14:143–51.
37. Kim J, Mcniff JM. Nuclear expression of survivin portends a poor prognosis in Merkel cell carcinoma. Mod Pathol 2008;21:764–9.
38. Ames HM, Bichakjian CK, Liu GY, Oravecz-Wilson KI, Fullen DR, Verhaegen M, et al. Huntingtin-interacting protein 1: a Merkel cell carcinoma marker that interacts with c-Kit. J Invest Dermatol 2011; 131:1–8.
39. Engelhardt B, Ransohoff RM. The ins and outs of T-lymphocyte trafficking to the CNS: anatomical sites and molecular mechanisms. Trends Immunol 2005;26:485–95.
40. Azimi F, Scolyer RA, Rumcheva P, Moncrieff M, Murali R, McCarthy SW, et al. Tumor-infiltrating lymphocyte grade is an independent predictor of sentinel lymph node status and survival in patients with cutaneous melanoma. J Clin Oncol 2012;30:2678–83.
41. Gooden MJ, de Bock GH, Leffers N, Daemen T, Nijman HW. The prognostic influence of tumour-infiltrating lymphocytes in cancer: a systematic review with meta-analysis. Br J Cancer 2011;105:93–103.
42. Afanasiev OK, Nagase K, Simonson W, Vandeven N, Blom A, Koelle DM, et al. Vascular E-selectin expression correlates with CD8 lymphocyte infiltration and improved outcome in Merkel cell carcinoma. J Invest Dermatol 2013;133:2065–73.
43. Ghebeh H, Barhoush E, Tulbah A, Elkum N, Al-Tweigeri T, Dermime S. FOXP3+ Tregs and B7-H1+/PD-1+ T lymphocytes co-infiltrate the tumor tissues of high-risk breast cancer patients: implication for immunotherapy. BMC Cancer 2008;8:57.
44. Poschke I, De Boniface J, Mao Y, Kiessling R. Tumor-induced changes in the phenotype of blood-derived and tumor-associated T cells of early stage breast cancer patients. Int J Cancer 2012;131:1611–20.

45. Sfanos KS, Bruno TC, Meeker AK, De Marzo AM, Isaacs WB, Drake CG. Human prostate-infiltrating CD8+ T lymphocytes are oligoclonal and PD-1+. Prostate 2009;69:1694–703.
46. Brahmer JR, Tykodi SS, Chow LQ, Hwu WJ, Topalian SL, Hwu P, et al. Safety and activity of anti-PD-L1 antibody in patients with advanced cancer. N Engl J Med 2012;366:2455–65.
47. Topalian SL, Hodi FS, Brahmer JR, Gettinger SN, Smith DC, McDermott DF, et al. Safety, activity, and immune correlates of anti-PD-1 antibody in cancer. N Engl J Med 2012;366: 2443–54.
48. Hodi FS, O'Day SJ, McDermott DF, Weber RW, Sosman JA, Haanen JB, et al. Improved survival with ipilimumab in patients with metastatic melanoma. N Engl J Med 2010;363:711–23.
49. Gomez BP, Wang C, Viscidi RP, Peng S, He L, Wu TC, et al. Strategy for eliciting antigen-specific CD8+ T cell-mediated immune response against a cryptic CTL epitope of Merkel cell polyomavirus large T antigen. Cell Biosci 2012;2:36.
50. Zeng Q, Gomez BP, Viscidi RP, Peng S, He L, Ma B, et al. Development of a DNA vaccine targeting Merkel cell polyomavirus. Vaccine 2012;30:1322–9.